The EMBO Journal vol.12 no.6 pp.2233-2239, 1993

Two-dimensional structure of the membrane domain of human Band 3, the anion transport protein of the erythrocyte membrane

D.N.Wang, W.Kühlbrandt, V.E.Sarabia[1] and R.A.F.Reithmeier[1,2]

European Molecular Biology Laboratory, Meyerhofstrasse 1, 6900 Heidelberg, Germany and [1]MRC Group in Membrane Biology, Departments of Medicine and Biochemistry, University of Toronto, Toronto, M5S 1A8, Canada

[2]Corresponding author

Communicated by P.N.T.Unwin

The membrane domain of human erythrocyte Band 3 protein (M_r 52 000) was reconstituted with lipids into two-dimensional crystals in the form of sheets or tubes. Crystalline sheets were monolayers with six-fold symmetry (layer group *p6*, $a = b = 170$ Å, $\gamma = 60°$), whereas the symmetry of the tubular crystals was *p2* ($a = 104$ Å, $b = 63$ Å, $\gamma = 104°$). Electron image analysis of negatively stained specimens yielded projection maps of the protein at 20 Å resolution. Maps derived from both crystal forms show that the membrane domain is a dimer of two monomers related by two-fold symmetry, with each monomer consisting of three subdomains. In the dimer, two subdomains of each monomer form a roughly rectangular core (40 × 50 Å in projection), surrounding a central depression. The third subdomain of the monomer measures ~15 × 25 Å in projection and appears to be connected to the other two by a flexible link. We propose that the central depression may represent the channel for anion transport while the third subdomain appears not to be directly involved in channel formation.

Key words: anion transport/Band 3/electron microscopy/membrane protein crystallization

Introduction

Human Band 3 or AE1 (AE for anion exchanger) is a 911 amino acid glycoprotein (Tanner *et al.*, 1988; Lux *et al.*, 1989) that mediates the electroneutral exchange of anions such as Cl^- and HCO_3^- across the erythrocyte membrane, an important step in CO_2 elimination (Passow, 1986; Jennings, 1989). Band 3 is a member of a multigene family (Alper, 1991) encoding membrane proteins involved in anion transport in a wide variety of cells. A truncated form of AE1 (Brosius *et al.*, 1989; Kudrycki and Schull, 1989) is found in the basolateral membrane of intercalated cells in the kidney, where it is responsible for bicarbonate reabsorption. AE2 (Demuth *et al.*, 1986; Alper *et al.*, 1988; Kudrycki *et al.*, 1990; Lindsey *et al.*, 1990) is a ubiquitous form of the transporter that plays an important role, along with the Na^+/H^+ exchanger, in maintaining intracellular pH (Alper, 1991). A third, neuronal form of Band 3 (AE3) is expressed in the brain and heart (Kopito *et al.*, 1989).

Band 3 consists of two domains that are structurally and functionally independent (Jennings, 1989). Mild trypsin treatment of ghost membranes cleaves Band 3 on the cytosolic side of the membrane at lysine 360, 45 amino acids from the beginning of the first transmembrane segment (Lepke and Passow, 1976; Steck *et al.*, 1976; Mawby and Findley, 1982). The amino-terminal cytosolic domain (M_r 43 000; Low, 1986) provides the attachment site for the cytoskeleton via ankyrin and Band 4.1 binding. The amino-terminus of Band 3 binds haemoglobin and glycolytic enzymes, regulating glycolysis by a novel phosphorylation/dephosphorylation mechanism (Low *et al.*, 1987). This domain is quite elongated and undergoes dramatic conformational changes in response to pH (Appell and Low, 1981). The carboxyl-terminal membrane domain (M_r 52 000) is fully capable of carrying out anion exchange (Lepke and Passow, 1976; Grinstein *et al.*, 1979). Consistent with its transport function, the membrane domain of Band 3 is thought to span the membrane with up to 14 transmembrane segments (Tanner, 1989). The transmembrane segments protected from proteolytic digestion by the membrane are entirely α-helical in conformation (Oikawa *et al.*, 1985). This domain contains a single site of asparagine-linked oligosaccharide that consists of a heterogeneous polylactosaminyl structure (Fukuda *et al.*, 1984). Enzymatic deglycosylation of Band 3 does not result in any major changes in protein structure and does not impair anion transport (Casey *et al.*, 1992). Band 3 is arranged as a mixture of dimers and tetramers in the membrane and in detergent solutions (Pappert and Schubert, 1983; Jennings, 1984; Casey and Reithmeier, 1991). However, the isolated membrane domain is exclusively dimeric (Casey and Reithmeier, 1991). The functional significance of various oligomeric states of Band 3 (Jennings, 1984) is still under investigation.

Due to the abundance of Band 3 in the erythrocyte membrane, this transporter has served as an excellent model system in the study of membrane protein structure. The facile purification of Band 3 has enabled extensive characterization of this protein in detergent solutions. Various studies have shown that Band 3 maintains its native structure in detergents such as octaethylene glycol *n*-dodecyl ether ($C_{12}E_8$) (Reithmeier *et al.*, 1989). Lipids containing long-chain saturated (eg. stearic) fatty acids remain tightly associated with Band 3 after purification (Maneri and Low, 1989) and these types of lipids are known to stabilize the membrane domain against thermal denaturation (Maneri and Low, 1988; Sami *et al.*, 1992).

In order to determine the mechanism of anion transport at the molecular level, a high resolution structure must be determined. Electron crystallographic analysis of membrane proteins such as bacteriorhodopsin (Henderson *et al.*, 1990), light harvesting complex (Kühlbrandt and Wang, 1991) and porins (Jap *et al.*, 1991) have given detailed structural information to relatively high resolution. We report here the formation of two types of crystalline arrays of the membrane domain of Band 3. Projection maps based on image analyses

of negatively stained two-dimensional crystals reveal the dimeric nature of the protein, a pore at the dimer interface and three subdomains within each monomer.

Results

Membrane domain of Band 3

Figure 1 is an SDS gel showing a typical preparation of the membrane domain of Band 3 produced by trypsin treatment of ghost membranes before and after deglycosylation. The membrane domain of human Band 3 is 551 amino acids in length and extends from Gly361 to the Val911, with a single oligosaccharide chain attached to Asp642. The glycosylated domain migrates as a broad band on SDS gels with a sharp leading edge at 52 000 and a trailing region that contains polylactosaminyl oligosaccharide (Casey *et al.*, 1992). The broad nature of the protein band is due to the heterogeneous nature of the oligosaccharide chain, since deglycosylation results in considerable sharpening of the band (Figure 1). The deglycosylated protein has an apparent molecular weight of 46 000 by SDS gel electrophoresis (Figure 1). Size exclusion high pressure liquid chromatography showed that the purified membrane domain in $C_{12}E_8$ eluted as a single peak with a Stokes radius of 68 Å, previously characterized as a dimer (Casey and Reithmeier, 1991).

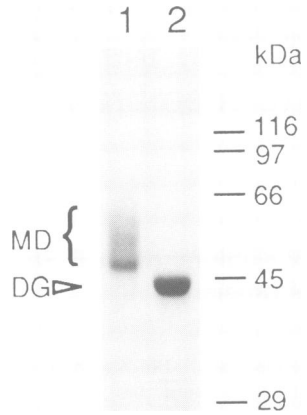

Fig. 1. Coomassie blue-stained SDS–polyacrylamide gel with of 5 μg of the purified membrane domain (MD, lane 1) and the deglycosylated membrane domain (DG, lane 2). Positions of molecular weight markers are indicated to the right of the gel, with molecular masses in kDa.

Crystallization

Samples of native and deglycosylated membrane domain were reconstituted with phospholipid and cholesterol, and negatively stained specimens were examined by electron microscopy. After 1–3 weeks, a number of samples showed tubular or two-dimensional crystals (Figure 2). These were most abundant when a combination of dimyristoyl phosphatidyl choline (DMPC) and cholesterol was used for reconstitution but phospholipids having shorter or longer fatty acid chains also yielded crystalline arrays.

The deglycosylated membrane domain produced sheet-like two-dimensional crystals (Figure 2a), as well as tubes. Sheets grew to a maximum size of 2 μm in diameter but most measured ~0.5–1 μm across. Judging from edge-on views (arrowhead in Figure 2a), the sheets were single layers. Optical diffraction indicated *p*6 symmetry, with $a = b =$ 170 Å and reflections extending to 20 Å. The crystalline sheets were always found on extensive layers of lipid. It is possible that the crystalline protein segregated into part of a large vesicle that bound to the carbon grid and then fractured upon binding or staining. However, their appearance suggests that they formed on a lipid bilayer which then attached to the carbon film. The symmetry of the optical diffraction patterns showed that all sheets faced the same way on the support grid, indicating that one side of the Band 3 membrane domain interacts preferentially with the lipid film.

The tubular crystals grown from protein solubilized in $C_{12}E_8$ and Triton X-100 had different diameters. Tubes grown from Triton X-100 measured ~650 Å across and were 1–3 μm long (Figure 2b). The most highly ordered specimens showed reflections to 18 Å resolution by optical diffraction. The diameter of the tubes grown from $C_{12}E_8$ varied between 1000 and 1500 Å (Figure 2c). These wider tubes were less well ordered, diffracting to ~27 Å resolution. Unlike the narrow tubes they frequently seemed to form a Y shape at one end. Even though their outside appearance was quite different, the lattice parameters and crystal packing of both kinds of tubes were the same. Upon negative staining, the tubes were flattened against the carbon support film. The two layers were treated as two separate two-dimensional crystals facing in opposite directions. The layer group of the flattened tubes was *p*2, with $a = 104$ Å, $b = 63$ Å, $\gamma = 104°$. The edges of both types of tubes were quite smooth, without any major surface protrusions.

Projection maps

Negatively stained tubular and two-dimensional crystals of the membrane domain were analysed by low dose electron microscopy and image processing. Several hundred micrographs were recorded and the best images were selected for computer processing. Seven crystalline areas from six images of crystalline sheets were processed, yielding an averaged projection map at 20 Å resolution (Figure 3a). The map shows that the protein crystallizes as a dimer, with the monomers related by a two-fold axis of symmetry. The dimensions of the dimer in sheets are 110 × 40 Å and each monomer had an L or 'dog-leg' shape. The unit cell contained three dimers, with their two-fold symmetry axes on the crystallographic two-fold axes and three dimers around a crystallographic three-fold axis. There was only one type of contact between dimers, resulting in a very open, mesh-like structure with lipid and residual detergent occupying at least 50% of the area.

Structure factors from four areas of three tubular crystals yielded another averaged projection map at 20 Å resolution (Figure 3b). As in the two-dimemsional sheets, the membrane domain crystallized as a dimer. The monoclinic unit cell contained one dimer, again with its two-fold symmetry axis on the crystallographic two-fold axis. The elongated dimers (120 × 35 Å) were arranged head to head in the *a* direction and side to side along the *b* direction, resulting in a fairly dense molecular packing, with ~70% of the area taken up by protein.

In both sheets and tubes, there is a stain-filled depression at the position of the two-fold axis in the centre of the dimer, suggesting that this is the channel through which the anions

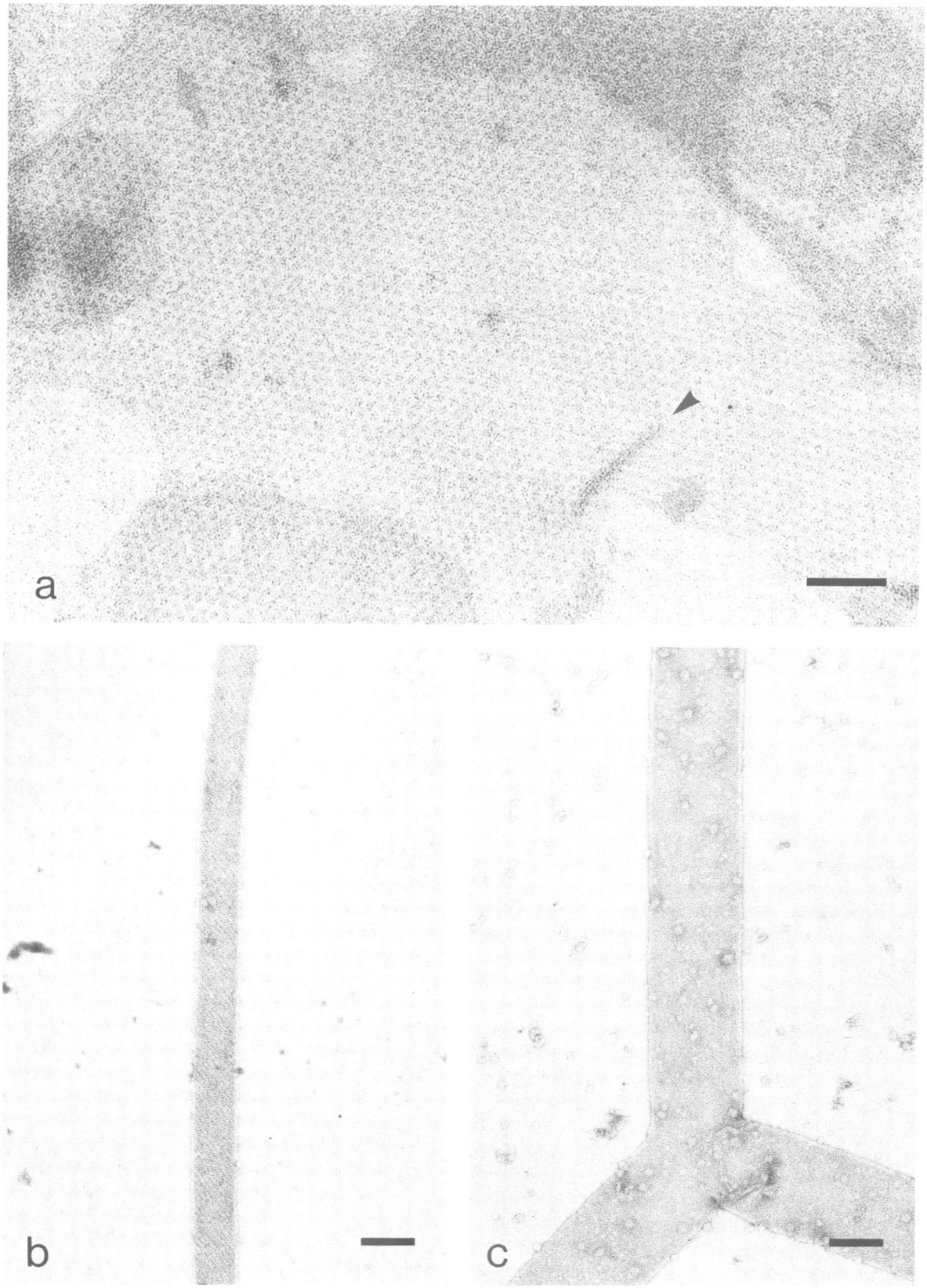

Fig. 2. Two-dimensional crystals of the reconstituted membrane domain of human Band 3, negatively stained with uranyl acetate. (**a**) Two-dimensional crystal of deglycosylated membrane domain of human erythrocyte Band 3 grown with $C_{12}E_8$ as a detergent. The arrowhead points to a fold in the sheet that indicates that the sheet is a monolayer. Double layers can be distinguished near the edge of the micrograph. (**b**) Narrow tube (650 Å diameter) of glycosylated membrane domain grown from Triton X-100 solution. (**c**) Wide tube (1500 Å diameter) of glycosylated membrane domain, grown from $C_{12}E_8$ solution. Wide tubes occasionally form a Y shape, as seen near the lower edge of this panel. Scale bars, 1000 Å.

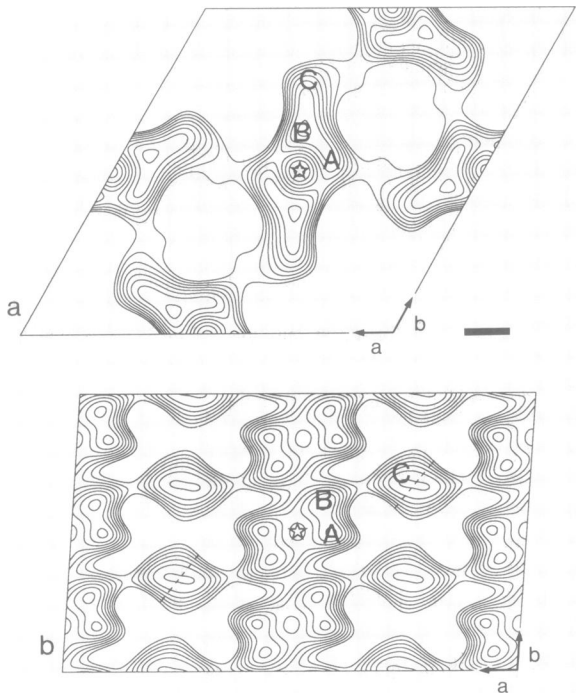

Fig. 3. Projection maps of negatively stained Band 3 membrane domain at 20 Å resolution. (**a**) Projection map of two-dimensional sheet with *p*6 symmetry. One unit cell is shown ($a = b = 170$ Å, $\gamma = 120°$). (**b**) Projection map of tubular crystals with *p*2 symmetry. An area of 2×3 unit cells is shown ($a = 104$ Å, $b = 63$ Å, $\gamma = 104°$). Both maps show that the protein is a dimer consisting of two identical monomers, related by two-fold symmetry. Each monomer consists of three subdomains, labelled A, B and C. At the interface between subdomains A and B from adjacent monomers there is a depression (asterisk) that probably represents the channel for anion transport. Note the different position of subdomain C with respect to A and B in the two crystal forms. The dashed lines in (b) mark the approximate dividing line between subdomains C from two dimers which are in contact at this site. Directions of unit cell vectors *a* and *b* are indicated. Scale bar, 20 Å.

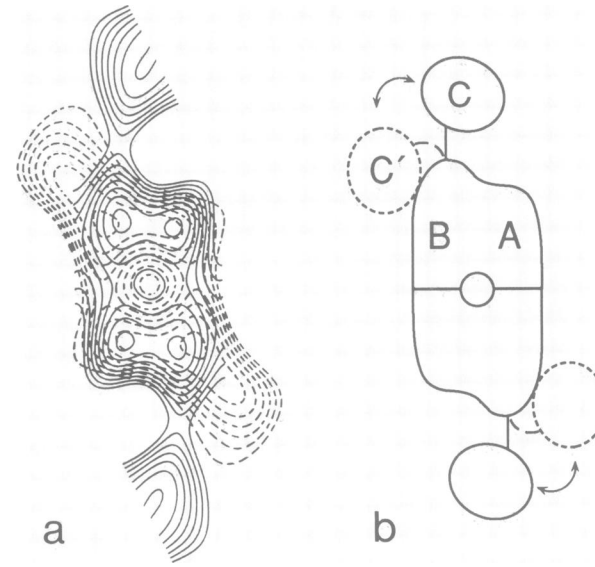

Fig. 4. (**a**) Superposition of the projection map of a single dimer from two-dimensional sheets (dashed) and tubular crystals (solid contours). The positions of the pore and of subdomains A and B coincide in both maps, whereas subdomain C changes position by ~30 Å.
(**b**) Schematic drawing, indicating the proposed flexible link between subdomain C and the central pore-forming core of the membrane domain, and suggesting how the protein may change from an extended to a more compact conformation.

are transported. This implies that the dimer is the functional unit of Band 3. Each monomer consists of three subdomains, labelled A, B and C in Figure 3. Two of these, A and B, appear to share a large surface at the dimer interface, producing a stable dimeric structure. Two pairs of domains A and B make up a roughly rectangular core of the dimer, measuring ~40 × 50 Å in projection (most clearly seen in the projection of tubes, Figure 3b). Between them, subdomains A and B appear to form a channel at the monomer interface. As can be seen in the superposition of the two projection maps (Figure 4a), the shape, size and position of subdomains A and B and of the central depression is very similar in both crystal forms. The position of the dimer interface drawn in Figure 4b is suggested by the contour lines in Figure 3a and b, which indicate a stronger connection across rather than along the central core of the dimer. The resulting shape of the monomer should, however, be regarded as tentative since the connections between subdomains A and B may prove to be different at higher resolution. The third subdomain, C, which measures ~15 × 25 Å in projection in tubes appears to be connected to the main body of the membrane domain by a flexible link allowing movement of subdomain C from a position adjacent to B in the crystalline sheet to a position ~30 Å away (Figure 4b). As a result, the dimer changes from a relatively compact structure (110 × 40 Å) in sheets to a more extended structure (120 × 35 Å) in tubes. The relative three-dimensional position of the subdomains can of course not be deduced from the projection maps. The smooth appearance of the edge of tubular crystals and of edge-on views of crystalline sheets suggests however that subdomain C is located in the plane of the membrane.

Discussion

Crystallization

Tubular and two-dimensional crystals were obtained after removal of the cytosolic domain of Band 3, with or without deglycosylation. Neither modification impairs the transport function of Band 3. It has been shown that the membrane domain of Band 3 is capable of carrying out anion transport in the absence of the cytosolic domain (Lepke and Passow, 1976; Grinstein *et al.*, 1979). Expression of the membrane domain of mouse Band 3 in *Xenopus laevis* oocytes has yielded a fully functional transporter (Lepke *et al.*, 1992). Similarly, expression of the membrane domain of AE3 in COS cells results in the production of a functional transporter (Kopito *et al.*, 1989). Removal of the oligosaccharide chain from Band 3 also does not impair its transport function (Casey *et al.*, 1991). We therefore believe that the structure of the membrane domain as determined by us is that of the functional transport protein.

Detergents such as $C_{12}E_8$ or Triton X-100 preserve the activity and native structure of Band 3 (Reithmeier *et al.*, 1989; Reithmeier and Casey, 1992). Sami *et al.* (1992) found that dodecyl chain detergent was optimal for stabilizing Band 3 against thermal denaturation. $C_{12}E_8$ therefore seems to be particularly suitable for maintaining the structure of Band 3 in solution and hence also for its crystallization. It is interesting to note that another ion transport membrane

protein, Ca^{2+}-ATPase, has also been crystallized from $C_{12}E_8$ and yielded both tubular and sheet-like crystals (Dux *et al.*, 1987; Taylor *et al.*, 1988; Stokes and Green, 1990).

The success of the two-dimensional crystallization depended to a large extent on the lipids used for reconstitution. We chose a mixture of DMPC and cholesterol because of the well-documented effects of these lipids on the protein. It is known that Band 3 reconstituted with phosphatidylcholine forms a fully functional transporter (Scheuring *et al.*, 1988) and that anion transport is not affected by cholesterol concentrations up to 27 mol% of total lipid (Kühne *et al.*, 1981). Phospholipids containing saturated fatty acids appear to stabilize the membrane domain (Maneri and Low, 1988) and phospholipids with zwitterionic head groups such as phosphatidyl choline (PC) have a greater stabilizing effect than the lipids with acidic head groups. The stabilizing effect of PC on the protein was very similar with myristic acid (C14:0), palmitoleic acid (C16:1) or linoleic acid (C18:2) as the fatty acid moiety. Cholesterol not only stabilizes the membrane domain of Band 3 (Maneri and Low, 1988), but has also been found to cause its aggregation within the membrane (Mühlebach and Cherry, 1982), which may be favourable for crystal formation.

The role of polyethylene glycol (PEG) in the crystallization is probably twofold, acting both as a protein precipitant and as an agent causing membrane fusion. Lentz *et al.* (1992) has observed that PEG induces fusion of unilamellar vesicles of dipalmitoyl PC in the presence of small amounts of an amphipathic compound such as lysolecithin. The role of low molecular weight PEG may be similar to that of glycerol in the two-dimensional crystallization of the plant light-harvesting complex where it is thought to disrupt the hydration shells around the detergent micelles, enabling them to merge into extensive lattices (Wang and Kühlbrandt, 1991). PEG has also also been used for growing two-dimensional crystals of alcohol oxidase on carbon film (Vonck and van Bruggen, 1990).

Dimer structure

The projection maps clearly show a dimer structure of the membrane domain of Band 3, arranged around a two-fold axis of symmetry. The interactions between monomers that results in dimer formation remains the same in all crystal forms. This shows that the dimer is the basic structural unit observed in these two-dimensional arrays. There is an extensive literature (Jennings, 1984) to support the existence of Band 3 dimers in detergent solution and in the membrane. Hydrodynamic studies of the purified membrane domain have shown that it exists as a dimer in $C_{12}E_8$ with a Stokes radius of 68 Å (Casey and Reithmeier, 1991). This is also the case for Band 3 reconstituted into sheets and tubes, therefore the membrane domain appears to retain its oligomeric state upon crystallization.

Transport channel

An important feature of the projection map is the presence of a stain-filled pore at the interface between two Band 3 subunits. It is known that Band 3 contains a binding site for stilbene disulfonates, potent inhibitors of anion transport (Cabanchik and Greger, 1992). Since these compounds are competitive inhibitors of transport, the stilbene disulfonate site may overlap the anion binding site. This site must be large enough to accommodate these large organic anions. There is one site per Band 3 molecule and access to this site is from the outside of the cell (Kaplan *et al.*, 1976). The large depression visible in the projection map may represent the stilbene disulfonate binding site or an access to the site. This implies that the inhibitor site may penetrate some distance into the protein. Indeed, immobilized anion transport inhibitors bind Band 3 only when attached to a carrier by a long flexible link (Pimplikar and Reithmeier, 1986; Eidelman *et al.*, 1991). Energy transfer experiments (Rao *et al.*, 1979) have shown that the stilbene disulfonate site is located some distance into the membrane. Inhibitor eosin maleimide when bound to Band 3 from the outside become inaccessible to quenchers of fluorescence (Macara *et al.*, 1983). A two-stage binding process has been observed for some inhibitors (Dix *et al.*, 1979; Verkman *et al.*, 1983), the second high affinity stage representing a sequestering of the inhibitor within the transport pathway. The bound inhibitors also stabilize the membrane domain against thermal denaturation (Snow *et al.*, 1978; Davio and Low, 1982; Oikawa *et al.*, 1985) and proteolysis (Kang *et al.*, 1992) suggesting extensive inhibitor−protein interactions.

There is evidence that the two binding sites within a dimer are in close contact. Energy transfer experiments have shown that the sites are within 28−52 Å of each other (Macara and Cantley, 1981) and that large stilbene disulfonates interact with one another (Dix *et al.*, 1979). Immobilized Band 3 monomers are unable to bind stilbene disulfonates, suggesting that a dimeric structure is required for inhibitor binding (Boodhoo and Reithmeier, 1984). Allosteric interactions between subunits have been suggested by the work of Salhany (1990). A transport pore may therefore be formed at the interface between two Band 3 molecules. This implies that the functional unit of Band 3 is a dimer. This conclusion contradicts the finding by Lindenthal and Schubert (1991) that isolated Band 3 monomers when reconstituted into small lipid vesicles are capable of transport.

Many of the known transport proteins are oligomers (Klingenberg, 1981). The subunits assemble into an approximately or perfectly symmetrical structure, forming a pore at the position of the symmetry axis (Unwin, 1989). The passage across the membrane is formed between subunits rather than within a single subunit. Channels consisting of 3−6 subunits have previously been observed. The structure of the Band 3 protein suggests that channels can also form from two symmetrical subunits. An oligomeric channel has the obvious advantage of being more economical with respect to genetic information but it also offers the potential of regulation by allosteric change, as is the case with other soluble and membrane proteins (Perutz, 1989).

In the Ca^{2+}-ATPase, surface projections correspond to a large cytosolic domain (Taylor *et al.*, 1988). In the preparation of the membrane domain of Band 3, a similar cytosolic domain was removed, which may account for the lack of surface projections. The lack of prominent surface projections is in agreement with current folding models of Band 3, which place 14 transmembrane helices ~21 residues in length (making up 60% of the membrane domain) in the bilayer joined by relatively short loops. Interestingly, circular dichroism measurements of the membrane domain show that it contains ~60% α-helix, with the transmembrane segments being entirely helical (Oikawa *et al.*, 1985). The remaining 40% of the structure likely consists of small loops connecting the transmembrane segments.

Subdomain structure

Two subdomains, A and B, form the central core of the membrane domain of Band 3 and seem to surround a pore. The presence of a third subdomain at some distance from the channel was unexpected. If the transport site is indeed at the interface between the Band 3 monomers, as the projection maps suggest, then subdomain C is unlikely to be itself involved forming the channel. A possible role for this part of the protein is that of a linker to the amino-terminal cytosolic domain of the protein. A flexible link within the membrane would isolate the transport domain of Band 3 from the rest of the molecule which is involved in binding to the cytoskeleton.

The different conformations observed in the two crystal forms may simply reflect an adaptation of the membrane domain to different packing constraints in the two crystal forms. Alternatively, the different crystal forms may be the result of a conformational change in response to deglycosylation or to slightly different crystallization conditions. The removal of the oligosaccharide chain may allow the Band 3 molecules to assume a different packing arrangement that is expressed as a change in the gross morphology to the crystal arrays, producing sheets rather than tubes. It is possible that the movement of the third domain induces a small rearrangement of subdomains A and B which may be significant in the transport mechanism.

In conclusion, our results show that the dimer is the fundamental structural unit of the transport domain of Band 3 protein, and that the channel for anion transport is probably located at the dimer interface. The protein can be crystallized in two dimensions in the absence of the cytosolic domain. With better crystals, a structure at higher resolution will be obtained.

Materials and methods

The membrane domain of Band 3 was prepared as described previously (Casey *et al.*, 1989). Briefly, ghost membranes were digested with trypsin (5 μg/ml) for 1 h on ice. The membranes were stripped of extrinsic fragments by treatment with 2 mM EDTA, pH 12. The membrane was dissolved in 1% $C_{12}E_8$ or Triton X-100 and the extract was chromatographed on a DEAE column, eluted with a linear gradient (0–500 mM) of NaCl in 0.1% $C_{12}E_8$ or Triton X-100 in 5 mM sodium phosphate, pH 8.0. The membrane domain eluted with 100 mM NaCl at a protein concentration of ~1 mg/ml. The protein was deglycosylated in the same buffer by incubation with 2 units/mg protein of *N*-glycosidase F (Boehringer Mannheim) at room temperature for 18 h (Casey *et al.*, 1992). The homogeneity of the samples was confirmed by SDS gel electrophoresis (Laemmli, 1970) and size exclusion high pressure liquid chromotography (Casey and Reithmeier, 1991).

The membrane domain of Band 3 was reconstituted with various phospholipids (dilauryl, dimyristoyl, dipalmitoyl and dioleyl PC) and cholesterol at different concentrations, and the detergent concentration was then lowered by microdialysis in glass capillaries, as described by Kühlbrandt (1992). Typically, 100 μg of purified membrane domain in 0.1% $C_{12}E_8$ or Triton X-100, 100 mM NaCl, 5 mM sodium phosphate, pH 8.0 were mixed with an equal weight of phospholipid and 5 μg cholesterol. Samples (100 μl) were dialysed at 27°C against 100 mM NaCl, 10 mM $MgCl_2$, 0.5 mM dithioerythritol, 0.5 mM sodium azide, 5 mM phosphate, pH 8.0 and 10% PEG 200, 300 or 400. Aliquots were taken at intervals of several days and examined by electron microscopy.

The EM grids were prepared by negative staining with 2% uranyl acetate. Low dose micrographs were recorded on a JEOL 2000EX electron microscope equipped with a Gatan image intensifier at magnification of 40 000× and developed with Kodak D19 developer at full strength for 12 min. The best images were selected by optical diffraction and areas of 1024×1024 or 2048×2048 image points were digitized on a Perkin–Elmer 1010M microdensitometer with a step size of 20 μm. Images were processed by established methods (Amos *et al.*, 1982) on a VAX computer cluster. Lattice distortions were corrected as described by Henderson *et al.* (1986). Projection maps were calculated with the CCP4 crystallographic programs.

Acknowledgements

Dr R.Poole and C.Landolt are thanked for their comments on the manuscript. This research was supported by an MRC of Canada Group Grant to R.A.F.R.

References

Alper,S.L. (1991) *Annu. Rev. Physiol.*, **53**, 549–564.
Alper,S.L., Kopito,R.R., Libresco,S.M. and Lodish,H.F. (1988) *J. Biol. Chem.*, **263**, 17092–17099.
Amos,L.A., Henderson,R. and Unwin,P.N.T. (1982) *Progr. Biophys. Mol. Biol.*, **39**, 183–231.
Appell,K.C. and Low,P.S. (1981) *J. Biol. Chem.*, **256**, 11104–11111.
Boodhoo,A. and Reithmeier,R.A.F. (1984) *J. Biol. Chem.*, **259**, 785–790.
Brosius,F.C., Alper,S.L., Garcia,A.M. and Lodish,H.F. (1989) *J. Biol. Chem.*, **264**, 7784–7787.
Cabantchik,Z.I. and Greger,R. (1992) *Am. J. Physiol.*, **31**.
Casey,J.R. and Reithmeier,R.A.F. (1991) *J. Biol. Chem.*, **266**, 15726–15737.
Casey,J.R., Lieberman,D.M. and Reithmeier,R.A.F. (1989) *Methods Enzymol.*, **173**, 494–512.
Casey,J.R., Pirraglia,C.A. and Reithmeier,R.A.F. (1992) *J. Biol. Chem.*, **267**, 11940–11948.
Davio,S.R. and Low,P.S. (1982) *Biochemistry*, **21**, 3585–3593.
Demuth,D.R., Showe,L.C., Ballantine,M., Palumbo,A., Fraser,P.J., Cioe,L., Rovera,G. and Curtis,P.J. (1986) *EMBO J.*, **5**, 1205–1214.
Dix,J.A., Verkman,A.S., Solomon,A.K. and Cantley,L.C. (1979) *Nature*, **282**, 520–522.
Dux,L., Pikula,S., Mullner,N. and Martonosi,A. (1987) *J. Biol. Chem.*, **262**, 6439–6442.
Eidelman,O., Yanai,P., Englert,H.C., Lang,H.G., Greger,R. and Cabantchik,Z.I. (1991) *Am. J. Physiol.*, **260**, C1094–C1103.
Fukuda,M., Dell,A., Oates,J.E. and Fukuda,M.N. (1984) *J. Biol. Chem.*, **259**, 8260–8273.
Grinstein,S., Ship,S. and Rothstein,A. (1979) *Biochim. Biophys. Acta*, **507**, 294–304.
Henderson,R., Baldwin,J.M., Downing,K.H., Lepault,J. and Zemlin,F. (1986) *Ultramicroscopy*, **19**, 147–178.
Henderson,R., Baldwin,J.M., Ceska,T.A., Zemlin,F., Beckman,E. and Downing,K.H. (1990) *J. Mol. Biol.*, **213**, 899–929.
Jap,B.K., Walian,P.J. and Gehring,K. (1991) *Nature*, **350**, 167–170.
Jennings,M.L. (1984) *J. Membr. Biol.*, **80**, 105–117.
Jennings,M.L. (1989) *Annu. Rev. Biophys. Chem.*, **18**, 397–430.
Kang,D., Okubo,K., Hamaski,N., Kuroda,N. and Shiraki,H. (1992) *J. Biol. Chem.*, **267**, 19211–19217.
Kaplan,J.H., Scorah,K., Fasold,H. and Passow,H. (1976) *FEBS Lett.*, **62**, 182–185.
Klingenberg,M. (1981) *Nature*, **290**, 449–454.
Kopito,R.R., Lee,B.S., Simmons,D.M., Lindsey,A.E., Morgans,C.W. and Schneider,K. (1989) *Cell*, **59**, 927–937.
Kudrycki,K.E. and Shull,G.E. (1989) *J. Biol. Chem.*, **264**, 8185–8192.
Kudrycki,K.E., Newman,P.R. and Shull,G.E. (1990) *J. Biol. Chem.*, **265**, 462–471.
Kühlbrandt,W. (1992) *Q. Rev. Biophys.*, **25**, 1–49.
Kühlbrandt,W. and Wang,D.N. (1991) *Nature*, **350**, 130–134.
Kühne,W., Haest,C.W.M. and Deuticke,B. (1981) *Biochim. Biophys. Acta*, **664**, 108–120.
Laemmli,U.K. (1970) *Nature*, **227**, 680–685.
Lentz,B.R., McIntyre,G.F., Parks,D.J., Yates,J.C. and Massenburg,D. (1992) *Biochemistry*, **31**, 2643–2653.
Lepke,S. and Passow,H. (1976) *Biochim. Biophys. Acta*, **455**, 353–370.
Lepke,S., Becker,A. and Passow,H. (1992) *Biochim. Biophys. Acta*, **1106**, 13–16.
Lindenthal,S. and Schubert,D. (1991) *Proc. Natl Acad. Sci. USA*, **88**, 6540–6544.
Lindsey,A.E., Schneider,K., Simmons,D.M., Baron,R., Lee,B.S. and Kopito,R.R. (1990) *Proc. Natl Acad. Sci. USA*, **87**, 5278–5282.
Low,P.S. (1986) *Biochim. Biophys. Acta*, **864**, 145–167.
Low,P.S., Allen,D.P., Zioncheck,T.F., Chari,P., Willardson,B.M., Geahlen,R.L. and Harrison,M.L. (1987) *J. Biol. Chem.*, **262**, 4592–4596.

Lux,S.E., John,K.M., Kopito,R.R. and Lodish,H.F. (1989) *Proc. Natl Acad. Sci. USA*, **86**, 9089–9093.
Macara,I.A. and Cantley,L.C. (1981) *Biochemistry*, **20**, 5095–5105.
Macara,I.A., Kuo,S. and Cantley,L.C. (1983) *J. Biol. Chem.*, **258**, 1785–1792.
Maneri,L.R. and Low,P.S. (1988) *J. Biol. Chem.*, **263**, 16170–16178.
Maneri,L.R. and Low,P.S. (1989) *Biochem. Biophys. Res. Commun.*, **159**, 1012–1019.
Mawby,W.J. and Findlay,J.B.C. (1982) *Biochem. J.*, **205**, 465–475.
Mühlebach,T. and Cherry,R.J. (1982) *Biochemistry*, **21**, 4225–4228.
Oikawa,K., Lieberman,D.M. and Reithmeier,R.A.F. (1985) *Biochemistry*, **24**, 2843–2848.
Pappert,G. and Schubert,D. (1983) *Biochim. Biophys. Acta*, **730**, 32–40.
Passow,H. (1986) *Rev. Physiol. Biochem. Pharmacol.*, **103**, 61–223.
Perutz,M. (1989) *Q. Rev. Biophys.*, **22**, 139–236.
Pimplikar,S.W. and Reithmeier,R.A.F. (1986) *J. Biol. Chem.*, **261**, 9770–9778.
Rao,A., Martin,P., Reithmeier,R.A.F. and Cantley,L.C. (1979) *Biochemistry*, **18**, 4505–4516.
Reithmeier,R.A.F. and Casey,J.R. (1992) *Progr. Cell Res.*, **2**, 181–190.
Reithmeier,R.A.F., Lieberman,D.M., Casey,J.R., Pimplikar,S.W., Werner,P.K., See,H. and Pirraglia,C.A. (1989) *Ann. NY Acad. Sci.*, **574**, 75–83.
Salhany,J.M. (1990) *Erythrocyte Band 3 Protein*. CRC Press, Boca Raton, FL.
Sami,M., Malik,S. and Watts,A. (1992) *Biochim. Biophys. Acta*, **1105**, 148–154.
Scheuring,U., Lindenthal,S., Grieshaber,G., Haase,W. and Schubert,D. (1988) *FEBS Lett.*, **227**, 32–34.
Snow,J.W., Brandt,J.F. and Low,P.S. (1978) *Biochim. Biophys. Acta*, **512**, 579–591.
Steck,T.L., Ramos,B. and Stapazon,E. (1976) *Biochemistry*, **15**, 1154–1161.
Stokes,D.L. and Green,N.M. (1990) *Biophys. J.*, **57**, 1–14.
Tanner,M.J.A. (1989) *Methods Enzymol.*, **173**, 423–432.
Tanner,M.J.A., Martin,P.G. and High,S. (1988) *Biochem. J.*, **256**, 703–712.
Taylor,K.A., Mullner,N., Pikula,S., Dux,L., Peracchia,C., Varga,S. and Martonosi,A. (1988) *J. Biol. Chem.*, **263**, 5287–5294.
Unwin,P.N.T. (1989) *Neuron*, **3**, 665–676.
Verkman,A.S., Dix,J.A. and Solomon,A.K. (1983) *J. Gen. Physiol.*, **81**, 421–449.
Vonck,J. and van Bruggen,E.F.J. (1990) *Biochim. Biophys. Acta*, **1038**, 74–79.
Wang,D.N. and Kühlbrandt,W. (1991) *J. Mol. Biol.*, **217**, 691–699.

Received on February 22, 1993; revised on March 17, 1993